α decays to ground and excited states of heavy deformed nuclei

V. Yu. Denisov and A. A. Khudenko
Institute for Nuclear Research, Prospect Nauki 47, 03680 Kiev, Ukraine
(Received 24 July 2009; published 8 September 2009)

The experimental data for α-decay half-lives to ground and excited states of deformed nuclei with $222 \leqslant A \leqslant 252$ and $88 \leqslant Z \leqslant 102$ are analyzed in the framework of the unified model for α decay and α capture. The branching ratios to excited states depend on the energy and the angular momentum of the α particle. The evaluated branching ratios for $0^+_{\mathrm{g.s.}} \to 0^+_{\mathrm{g.s.}}, 2^+, 4^+$ α transitions in even-even nuclei agree with the experimental data. The experimental and calculated branching ratios for α transitions into more highly excited states are similar.

DOI: 10.1103/PhysRevC.80.034603 PACS number(s): 23.60.+e, 24.10.−i, 27.90.+b

I. INTRODUCTION

α decay is an important process in nuclear physics, therefore it has been extensively studied both experimentally and theoretically [1–26]. There are many experimental data for the α-decay half-lives between the ground states of nuclei, which have been discussed in the framework of various approaches [8–18]. Nuclei have many excited states of various natures, therefore α decay can take place from the ground or excited state of the parent nucleus to the ground or excited state of the daughter nucleus. The α transitions between the ground state of the parent nucleus and the excited state of the daughter nucleus have been widely discussed [4,6,7,19–25]. It is very important to study such transitions experimentally to build the energy-level schema of the daughter nucleus [27]. The α-decay rates for transitions between various states of parent and daughter nuclei are very different [1–4] due to energy and momentum dependencies of α decay. Furthermore, the structure of nuclear states also affects the rate.

The α-decay half-lives for transitions between ground states in 344 nuclei and the α-capture cross sections of ^{40}Ca, ^{44}Ca, ^{59}Co, ^{208}Pb, and ^{209}Bi have recently been well described in the framework of the unified model for α decay and α capture (UMADAC) [17]. In the framework of this model, α decay and α capture are considered as the penetration of the α particle through the potential barrier formed by nuclear, Coulomb, and centrifugal interactions between the α particle and nucleus. The spins and the parities of parent and daughter nuclei as well as the quadrupole and hexadecapole deformations of daughter nuclei are taken into account for evaluation of the α-decay half-lives.

Now we apply this model to the description of the α-decay branching ratios in various states of daughter nuclei. Transitions between the ground state of the parent nucleus and various nature excited states of the daughter nuclei can be considered in the framework of our approach in the case when (i) the formation of the α particle and daughter nucleus in the excited state is similar to that in the ground state, and (ii) the shape of the daughter nucleus in the excited state is the same as that in the ground state.

That is why the best candidates for application of our approach are the α decays into the low-lying rotational excited states of daughter nuclei, because such α transitions are simply affected by spins of α transitions. However, we carefully apply our model to α decays into excited states of other natures and determine the hindrance factors.

We propose that the shape of the daughter nucleus, both nuclear and Coulomb parts of the α-nucleus potential, are the same as the ones for the ground state of the daughter nucleus. In this case, we can use the same parameters of nuclear surface deformation as for the ground state. Therefore the branching ratios to excited states are determined by the α-decay energy and the angular momentum of the emitted α particle only. Using this proposal, we evaluate the branching ratios without introducing additional fitting parameters into our model [17].

The short description of the UMADAC [17] is given in Sec. II. Discussion of results is presented in Sec. III, and we make conclusions at the end.

II. UNIFIED MODEL FOR α DECAY AND α CAPTURE

The cluster approach is applied for the α decay between ground states of parent and daughter nuclei in the framework of the UMADAC [17]. The α-decay half-life $T_{1/2}(Q_i,\ell)$ is calculated as

$$T_{1/2}(Q_i,\ell) = \hbar \ln(2)/\,\Gamma(Q_i,\ell), \tag{1}$$

where $\Gamma(Q_i,\ell)$ is the width of decay

$$\Gamma(Q_i,\ell) = \hbar 10^{\nu} P(Q_i,\ell). \tag{2}$$

Here ν is the assault frequency of collision of α particle with barrier, which also includes the probability of the parent nucleus representation as the α particle and daughter nucleus (preformation factor); $P(Q_i,\ell)$ is the α-nucleus potential, which determines the probability of subbarrier tunneling of the α particle; Q_i is the energy released at α decay; and ℓ is the angular momentum of the α transition. The expressions for these quantities are given in Ref. [17].

We now consider α decays from the ground state of the parent nucleus into the ground and excited states of the daughter nucleus. We propose that the probability of parent nucleus representation as the α particle and daughter nucleus in the excited state is the same as the one for the α particle and daughter nucleus in the ground state. Therefore the assault frequency is the same in both cases, and we can apply Eq. (20)

from Ref. [17] for the assault frequency for all transitions into any state of the daughter nucleus.

The excited states of daughter nuclei have different energies and quantum numbers. Due to this, we discuss briefly the quantities related to the evaluation of the probability of subbarrier tunneling of the α particle at α decay in the framework of UMADAC. The tunneling probability of the α particle under the barrier formed by the interaction potential between the α particle and the axially symmetric deformed daughter nucleus is given as

$$P(Q_i,\ell) = \frac{1}{2}\int_0^{\pi} d\theta \sin\theta\, t(Q_i,\theta,\ell), \tag{3}$$

where θ is the angle of α emission relative to the symmetry axis of the daughter nucleus. Note that α emission can occur in any direction. We evaluate the transmission coefficient in the semiclassical WKB approximation

$$t(Q_i,\theta,\ell) = 1\bigg/\left\{1+\exp\left[\frac{2}{\hbar}\int_{a(\theta)}^{b(\theta)} dr\sqrt{2\mu(v(r,\theta,\ell,Q_i)-Q_i)}\right]\right\}. \tag{4}$$

Here μ is the reduced mass, $a(\theta)$ and $b(\theta)$ are the inner and outer turning points for the α particle emitted on angle θ relative to the symmetry axis of the daughter nucleus. The α-nucleus potential $v(r,\theta,\ell,Q_i)$ consists of Coulomb $v_C(r,\theta)$, nuclear $v_N(r,\theta,Q_i)$, and centrifugal $v_\ell(r)$ parts [17]

$$v(r,\theta,\ell,Q_i) = v_C(r,\theta) + v_N(r,\theta,Q_i) + v_\ell(r), \tag{5}$$

where

$$v_C(r,\theta) = \frac{2Ze^2}{r}\left[1+\frac{3R^2}{5r^2}\beta_2 Y_{20}(\theta) + \frac{3R^4}{9r^4}\beta_4 Y_{40}(\theta)\right] \tag{6}$$

for $r \geqslant r_m(\theta)$,

$$v_C(r,\theta) \approx \frac{2Ze^2}{r_m(\theta)}\left[\frac{3}{2}-\frac{r^2}{2r_m(\theta)^2}+\frac{3R^2}{5r_m(\theta)^2}\beta_2 Y_{20}(\theta) \times\left(2-\frac{r^3}{r_m(\theta)^3}\right)+\frac{3R^4}{9r_m(\theta)^4}\beta_4 Y_{40}(\theta)\left(\frac{7}{2}-\frac{5r^2}{2r_m(\theta)^2}\right)\right] \tag{7}$$

for $r \leqslant r_m(\theta)$,

$$v_N(r,\theta,Q_i) = \frac{V(Q_i)}{1+\exp[(r-r_m(\theta))/d]}, \tag{8}$$

$$v_\ell(r) = \frac{\hbar^2\ell(\ell+1)}{2\mu r^2}. \tag{9}$$

Here Z, R, β_2, and β_4 are, respectively, the number of protons, the radius, the quadrupole and hexadecapole deformation parameters of the nucleus interacting with the α particle; e is the charge of proton, $Y_{20}(\theta)$ and $Y_{40}(\theta)$ are the harmonic functions; $V(Q_i)$ and $r_m(\theta)$ are, correspondingly, the strength and the effective radius of the nuclear part of the α-nucleus potential. Presentation of the Coulomb field in the form (5) at distances $r \lesssim r_m(\theta)$ ensures the continuity of the Coulomb field and its derivative at matching point $r = r_m(\theta)$. The expressions for $V(Q_i)$,$r_m(\theta)$, and d are given in Ref. [17].

The α-particle emission from nuclei obeys the spin-parity selection rule. Let I_j, π_j and I_i, π_i be the spin and parity values of the parent nucleus in state j and the spin and parity values of the daughter nucleus in state i, respectively. Therefore the angular momentum of the emitted α particle satisfies the conditions

$$|I_j - I_i| \leqslant \ell_\alpha \leqslant I_j + I_i, \quad \frac{\pi_j}{\pi_i} = (-1)^{\ell_\alpha}, \tag{10}$$

because the α-particle spin and parity are $\pi_\alpha = +1$ and $I_\alpha = 0$, respectively.

The energy released in α decay between the ground states of parent and daughter nuclei is calculated using a recent evaluation of atomic mass data [2]. The effect of atomic electrons on the energy of the α particle should be also taken into account. Therefore the released energy of the α particle ($Q_{\text{g.s.}\to\text{g.s.}}$), emitted at transition between ground states of the parent and daughter nuclei, is [17]

$$Q_{\text{g.s.}\to\text{g.s.}} = \Delta M_p - (\Delta M_d + \Delta M_\alpha) + k\left(Z_p^\epsilon - Z_d^\epsilon\right), \tag{11}$$

where ΔM_p, ΔM_d and ΔM_α are, correspondingly, the mass-excess of parent, daughter and α nuclei. The last term in Eq. (11) describes the effect of atomic electrons, kZ^ϵ represents the total binding energy of Z electrons in the atom, where $k = 8.7$ eV and $\epsilon = 2.517$ for nuclei with $Z \geqslant 60$; and $k = 13.6$ eV and $\epsilon = 2.408$ for nuclei with $Z < 60$ [17,28].

The energy released in α transition between the level of parent nucleus with excitation energy E_{jp} and the level of daughter nucleus with excitation energy E_{id} is

$$Q_{j\to i} = Q_{\text{g.s.}\to\text{g.s.}} + E_{jp} - E_{id}. \tag{12}$$

We illustrate transition of similar type in Fig. 1. As one can see, the energy released at α decay from the ground state of the parent nucleus into the exited state i of the daughter nucleus with energy E_{id} is

$$Q_i \equiv Q_{0\to i} = Q_{\text{g.s.}\to\text{g.s.}} - E_{id}. \tag{13}$$

The branching ratio of the α decay from the ground state of the parent nucleus into level i of the daughter nucleus is

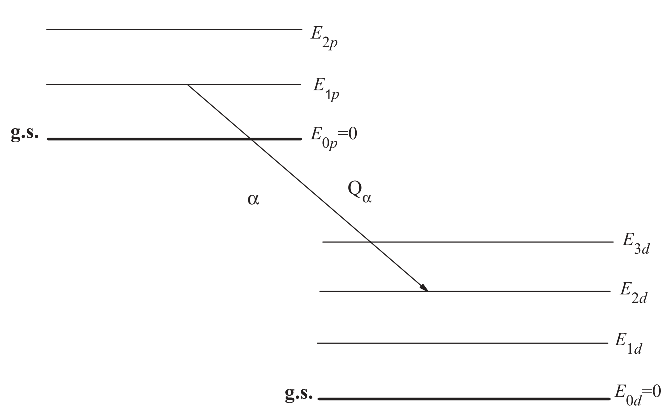

FIG. 1. α transition between the first excited state of parent nucleus with energy E_{1p} and the second exited state of daughter nucleus with energy E_{2d}.

determined as

$$B_i = \frac{\Gamma(Q_i,\ell_i)}{\sum_n \Gamma(Q_n,\ell_n)} \times 100\% = \frac{P(Q_i,\ell_i)}{\sum_n P(Q_n,\ell_n)} \times 100\%, \tag{14}$$

where the sum n is going over all states, which can be populated during the α transition from the ground state of the parent nucleus. The branching ratio is only related to the penetration factors in the framework of our approach.

The experimental data for the branching ratios for various nuclei and levels are presented in Refs. [1,4].

III. INPUT DATA

Starting from the ^{222}Ra, we examine the α transitions from ground into ground and excited states in 35 isotopes up to ^{252}No. Data of the α-decay branch ratios, energy values of the daughter exited levels, and spins and parities were extracted from the NuDat database [1].

The deformation of the daughter nucleus influences the total α-decay width [12,17,23]. Therefore the Coulomb and nuclear potentials [see Eqs. (5)–(8)] take into account the quadrupole and hexadecapole deformations of the daughter nucleus. We use the experimental deformation parameter values [3], except for the cases in which there are only theoretical ones, which we pick up from Ref. [8]. We propose that the shape of the nucleus at low excitation energy coincides with the ground-state one, therefore we consider the same values of deformation parameter for the ground and excited states. The values of deformation parameters β_2, β_4 for 35 isotopes considered in the paper are listed in Table I.

TABLE I. Values of deformation parameters β_2, β_4 for daughter nuclei.

Nuclei	β_2	β_4	Nuclei	β_2	β_4
$^{218}_{86}$Rn	0.0400	0.0290	$^{238}_{92}$U	0.2150	0.0930
$^{220}_{86}$Rn	0.1266	0.0810	$^{240}_{92}$U	0.2240	0.0790
$^{222}_{86}$Rn	0.1419	0.1000	$^{234}_{94}$Pu	0.2160	0.1090
$^{222}_{88}$Ra	0.1920	0.0920	$^{236}_{94}$Pu	0.2150	0.1100
$^{224}_{88}$Ra	0.1790	0.1120	$^{238}_{94}$Pu	0.2861	0.1020
$^{226}_{88}$Ra	0.2022	0.1120	$^{240}_{94}$Pu	0.2891	0.0870
$^{228}_{88}$Ra	0.2170	0.1130	$^{242}_{94}$Pu	0.2917	0.0710
$^{224}_{90}$Th	0.1640	0.1120	$^{244}_{94}$Pu	0.2931	0.0620
$^{226}_{90}$Th	0.2280	0.1110	$^{240}_{96}$Cm	0.2970	0.0870
$^{228}_{90}$Th	0.2301	0.1120	$^{242}_{96}$Cm	0.2240	0.0790
$^{230}_{90}$Th	0.2441	0.1150	$^{244}_{96}$Cm	0.2972	0.0730
$^{231}_{90}$Th	0.1980	0.1150	$^{246}_{96}$Cm	0.2983	0.0570
$^{232}_{90}$Th	0.2608	0.1080	$^{248}_{96}$Cm	0.2972	0.0400
$^{234}_{90}$Th	0.2410	0.1020	$^{244}_{98}$Cf	0.2340	0.0730
$^{230}_{92}$U	0.2620	0.1150	$^{246}_{98}$Cf	0.2340	0.0570
$^{232}_{92}$U	0.2640	0.1170	$^{248}_{98}$Cf	0.2350	0.0400
$^{234}_{92}$U	0.2718	0.1100	$^{248}_{100}$Fm	0.2350	0.0490
$^{236}_{92}$U	0.2821	0.1020			

IV. RESULTS

The experimental and calculated branching ratios of the α decay from the ground state of the parent nucleus into various levels of the daughter nucleus are presented in Table II. The branching ratio values are evaluated in the framework of our model by using Eqs. (3)–(14). The parameters of α-nucleus potential are listed in Ref. [17]. The values of deformation parameter for daughter nuclei used for α-nucleus potential evaluation are given in Table I. The first column of Table II shows the transition between initial and final states of nuclei. If the experimental spin-parity values of the nucleus are defined inaccurately, we enclose them in brackets. The second and third columns contain the calculated Q values and the minimal possible values of the orbital momentum of the α particle $\ell_{\min}$, correspondingly. For the sake of simplicity, we equate the value of the α-particle orbital momentum to the minimal possible value according to the rule of Eq. (10). The next two columns are the experimental and theoretical values of the branching ratios, respectively. Columns five and six are, correspondingly, the experimental $T^{\rm exp}_{1/2,i}$ and theoretical $T^{\rm theor}_{1/2,i}$ values of the α-decay half-lives. The hindrance factor

$$\mathrm{HF} = \frac{T^{\rm exp}_{1/2,i}}{T^{\rm theor}_{1/2,i}} \tag{15}$$

is given in the last column.

Note that experimental information on spin-parity values of daughter nucleus is absent in several cases. We propose that the minimal possible value of the orbital momentum of the α particle is zero ($\ell_{\min} = 0$) in such cases.

Comparing experimental and theoretical values of the branching ratios and half-lives presented in Table II, we can conclude that these values for transitions between ground states with angular momentum of α particle $\ell = 0$ and ground state to first excited state with $\ell = 2$ agree well. The theoretical values of the branching ratios for transitions with $\ell = 4$ overestimate the corresponding experimental ones as a rule. Note that similar results for transitions with $\ell = 4$ are obtained in Refs. [7,20,25], see also in Table III.

The quality of description of both the branching ratios and the half-lives is reduced with rising ℓ value, because our model is too simple and does not take into account various nuclear structure effects and fine mechanisms of α-particle formation in the parent nucleus. The preformation factor is reduced with rising ℓ value, thus the influence of nuclear structure and the mechanisms of α-particle formation on α decay is increased for high values of ℓ. By using the HF values, we obtain the numerical estimation of these effects, see also Tables II and III. The simple expressions of the Preston model [7] are often applied for estimation of the HF for α-decay transitions with $\ell = 0, 1, 2, 3, 4$ [4], but the HF for transitions with any value of ℓ can be estimated in the framework of our model.

By using values in Table II, we can easily estimate the HF for α transitions into excited states with $\ell \gtrsim 4$. We see that the HF is close to 10^0–10^1 for transitions into low-lying exited states with $\ell = 4, 5$ and to 10^2–10^3 for ones into high exited states of the daughter nucleus with the same values of

TABLE II. Comparison of the experimental and theoretical branch ratios and half-lives values.

Transition	Q	$\ell_{\min}$	$B^{\exp}(\%)$	$B^{\text{theor}}(\%)$	$T_{1/2}^{\exp}(\text{s})$	$T_{1/2}^{\text{theor}}(\text{s})$	HF
${}^{222}_{88}\text{Ra} \to {}^{218}_{86}\text{Rn}$							
$0^+ \to 0^+$	6.7136	0	96.90	96.70	37.3	47.5	0.79
$0^+ \to 2^+$	6.3896	2	3.05	3.27	1.19×10^3	1.40×10^3	0.84
$0^+ \to (4^+)$	6.0608	4	4.10×10^{-3}	6.34×10^{-2}	8.82×10^5	7.25×10^4	12.2
$0^+ \to (3^-)$	5.9170	3	4.10×10^{-3}	2.29×10^{-4}	8.82×10^5	2.01×10^7	4.40×10^{-2}
$0^+ \to (3^-)$	5.8737	3	4.20×10^{-3}	1.38×10^{-4}	8.61×10^5	3.34×10^7	2.58×10^{-2}
${}^{224}_{88}\text{Ra} \to {}^{220}_{86}\text{Rn}$							
$0^+ \to 0^+$	5.8242	0	94.92	95.70	3.33×10^5	1.18×10^6	0.28
$0^+ \to 2^+$	5.5832	2	5.06	4.22	6.25×10^6	2.68×10^7	0.23
$0^+ \to 4^+$	5.2905	4	7.30×10^{-3}	5.96×10^{-2}	4.33×10^9	1.90×10^9	2.28
$0^+ \to 1^-$	5.1788	1	7.60×10^{-3}	3.03×10^{-4}	4.16×10^9	3.74×10^{11}	1.11×10^{-2}
$0^+ \to (3^-)$	5.1612	3	3.00×10^{-3}	1.78×10^{-4}	1.05×10^{10}	6.35×10^{11}	1.66×10^{-2}
${}^{226}_{88}\text{Ra} \to {}^{222}_{86}\text{Rn}$							
$0^+ \to 0^+$	4.9058	0	94.45	95.80	5.35×10^{10}	1.90×10^{11}	0.28
$0^+ \to 2^+$	4.7196	2	5.55	4.18	9.10×10^{11}	4.36×10^{12}	0.21
$0^+ \to 4^+$	4.4574	4	6.50×10^{-3}	0.03	7.77×10^{14}	5.80×10^{14}	1.34
$0^+ \to 1^-$	4.3051	1	1.00×10^{-3}	4.61×10^{-5}	5.05×10^{15}	3.95×10^{17}	1.28×10^{-2}
$0^+ \to 3^-$	4.2703	3	2.70×10^{-4}	1.80×10^{-5}	1.87×10^{16}	1.01×10^{18}	1.85×10^{-2}
${}^{226}_{90}\text{Th} \to {}^{222}_{88}\text{Ra}$							
$0^+ \to 0^+$	6.4876	0	75.50	76.40	2.43×10^3	3.79×10^3	0.64
$0^+ \to 2^+$	6.3765	2	22.80	21.40	8.04×10^3	1.35×10^4	0.59
$0^+ \to 1^-$	6.2455	1	1.26	0.09	1.46×10^5	3.39×10^6	4.29×10^{-2}
$0^+ \to 4^+$	6.1862	4	0.19	2.06	9.81×10^5	1.41×10^5	6.98
$0^+ \to 3^-$	6.1703	3	0.21	3.04×10^{-2}	8.90×10^5	9.53×10^6	9.34×10^{-2}
$0^+ \to (5^-)$	6.0138	5	2.30×10^{-4}	3.55×10^{-3}	7.97×10^8	8.16×10^7	9.77
$0^+ \to (0^+)$	5.5736	0	3.40×10^{-4}	2.05×10^{-3}	5.39×10^8	1.41×10^8	3.82
$0^+ \to 2^+$	5.4627	2	1.70×10^{-4}	4.14×10^{-4}	1.08×10^9	6.99×10^8	1.54
${}^{228}_{90}\text{Th} \to {}^{224}_{88}\text{Ra}$							
$0^+ \to 0^+$	5.5565	0	72.20	76.30	8.36×10^7	1.35×10^8	0.62
$0^+ \to 2^+$	5.4721	2	27.20	21.90	2.22×10^8	4.71×10^8	0.47
$0^+ \to 1^-$	5.3405	1	0.42	0.06	1.44×10^{10}	1.73×10^{11}	8.29×10^{-2}
$0^+ \to 4^+$	5.3057	4	0.23	1.65	2.66×10^{10}	6.26×10^9	4.24
$0^+ \to (3)^-$	5.2661	3	3.80×10^{-2}	1.68×10^{-2}	1.59×10^{11}	6.16×10^{11}	0.26
$0^+ \to (5)^-$	5.1234	5	1.00×10^{-5}	1.41×10^{-3}	6.03×10^{14}	7.31×10^{12}	82.6
$0^+ \to (6^+)$	5.0772	6	2.50×10^{-5}	3.64×10^{-2}	2.41×10^{14}	2.84×10^{11}	8.50×10^2
$0^+ \to 0^+$	4.6402	0	1.80×10^{-5}	8.30×10^{-5}	3.35×10^{14}	1.25×10^{14}	2.69
$0^+ \to (2^+)$	4.5638	2	4.70×10^{-6}	1.89×10^{-5}	1.28×10^{15}	5.47×10^{14}	2.35
${}^{230}_{90}\text{Th} \to {}^{226}_{88}\text{Ra}$							
$0^+ \to 0^+$	4.8065	0	76.30	76.70	3.12×10^{12}	5.44×10^{12}	0.57
$0^+ \to 2^+$	4.7388	2	23.40	21.90	1.02×10^{13}	1.91×10^{13}	0.53
$0^+ \to 4^+$	4.5950	4	0.12	1.36	1.98×10^{15}	3.07×10^{14}	6.45
$0^+ \to 1^-$	4.5528	1	0.03	1.46×10^{-2}	7.93×10^{15}	2.87×10^{16}	0.276
$0^+ \to 3^-$	4.4850	3	9.70×10^{-4}	3.41×10^{-3}	2.45×10^{17}	1.22×10^{17}	2.00
$0^+ \to 6^+$	4.3900	6	8.00×10^{-6}	0.02	2.97×10^{19}	2.11×10^{16}	1.41×10^3
$0^+ \to 5^-$	4.3602	5	1.03×10^{-5}	2.20×10^{-4}	2.31×10^{19}	1.89×10^{18}	12.2
$0^+ \to 0^+$	3.9819	0	3.40×10^{-6}	1.36×10^{-5}	7.00×10^{19}	3.08×10^{19}	2.27
$0^+ \to 2^+$	3.9328	2	1.40×10^{-6}	3.96×10^{-6}	1.70×10^{20}	1.05×10^{20}	1.61
${}^{232}_{90}\text{Th} \to {}^{228}_{88}\text{Ra}$							
$0^+ \to 0^+$	4.1180	0	78.20	81.00	5.67×10^{17}	1.30×10^{18}	0.44
$0^+ \to 2^+$	4.0542	2	21.70	18.40	2.04×10^{18}	5.69×10^{18}	0.36
$0^+ \to 4^+$	3.9133	4	6.9×10^{-2}	0.61	6.43×10^{20}	1.72×10^{20}	3.74
${}^{228}_{92}\text{U} \to {}^{224}_{90}\text{Th}$							
$0^+ \to 0^+$	6.8418	0	69.40	71.30	8.03×10^2	9.27×10^2	0.87
$0^+ \to 2^+$	6.7488	2	28.60	25.70	1.95×10^3	2.57×10^3	0.76

TABLE II. (*Continued.*)

Transition	Q	ℓ_{min}	$B^{exp}(\%)$	$B^{theor}(\%)$	$T_{1/2}^{exp}(s)$	$T_{1/2}^{theor}(s)$	HF
$0^+ \to 1^-$	6.5958	1	0.65	0.09	8.53×10^4	7.41×10^5	0.12
$0^+ \to 4^+$	6.5618	4	0.56	2.97	9.93×10^4	2.22×10^4	4.47
$^{230}_{92}U \to ^{226}_{90}Th$							
$0^+ \to 0^+$	6.0308	0	67.40	68.80	2.67×10^6	2.48×10^6	1.07
$0^+ \to 2^+$	5.9586	2	32.00	26.20	5.62×10^6	6.51×10^6	0.86
$0^+ \to 4^+$	5.8044	4	0.38	3.09	4.73×10^8	5.53×10^7	8.55
$0^+ \to 1^-$	5.8004	1	0.26	0.06	6.91×10^8	2.79×10^9	0.25
$0^+ \to 3^-$	5.7233	3	1.15×10^{-2}	1.92×10^{-2}	1.56×10^{10}	8.90×10^9	1.76
$0^+ \to ?$	5.6798	0	5.40×10^{-4}	0.92	3.33×10^{11}	1.85×10^8	1.80×10^3
$0^+ \to ?$	5.6688	0	1.00×10^{-4}	0.80	1.80×10^{12}	2.13×10^8	8.45×10^3
$0^+ \to 6^+$	5.5835	6	7.00×10^{-5}	0.12	2.57×10^{12}	1.43×10^9	1.80×10^3
$0^+ \to 5^-$	5.5803	5	2.50×10^{-4}	2.13×10^{-3}	7.19×10^{11}	8.01×10^{10}	8.97
$0^+ \to (0^+)$	5.2256	0	3.00×10^{-4}	1.81×10^{-3}	5.99×10^{11}	9.44×10^{10}	6.34
$0^+ \to (2^+)$	5.1830	2	6.90×10^{-5}	8.54×10^{-4}	2.60×10^{12}	2.00×10^{11}	13.0
$^{232}_{92}U \to ^{228}_{90}Th$							
$0^+ \to 0^+$	5.4513	0	68.15	69.00	3.19×10^9	3.39×10^9	0.94
$0^+ \to 2^+$	5.3935	2	31.55	27.60	6.89×10^9	8.49×10^9	0.812
$0^+ \to 4^+$	5.2645	4	0.30	3.34	7.25×10^{11}	7.00×10^{10}	10.3
$0^+ \to 1^-$	5.1233	1	6.16×10^{-3}	8.78×10^{-3}	3.53×10^{13}	2.66×10^{13}	1.32
$0^+ \to 6^+$	5.0731	6	5.10×10^{-5}	0.12	4.26×10^{15}	1.89×10^{12}	2.25×10^3
$0^+ \to 3^-$	5.0552	3	4.80×10^{-5}	2.53×10^{-3}	4.53×10^{15}	9.24×10^{13}	49.0
$0^+ \to 5^-$	4.9321	5	5.60×10^{-5}	2.53×10^{-4}	3.88×10^{15}	9.25×10^{14}	4.20
$0^+ \to 0^+$	4.6195	0	2.10×10^{-5}	1.60×10^{-4}	1.04×10^{16}	1.46×10^{15}	7.09
$0^+ \to 2^+$	4.5768	2	3.90×10^{-6}	6.56×10^{-5}	5.58×10^{16}	3.57×10^{15}	15.6
$^{234}_{92}U \to ^{230}_{90}Th$							
$0^+ \to 0^+$	4.8954	0	71.38	71.00	1.09×10^{13}	1.00×10^{13}	1.08
$0^+ \to 2^+$	4.8422	2	28.42	26.40	2.73×10^{13}	2.70×10^{13}	1.01
$0^+ \to 4^+$	4.7213	4	0.20	2.60	3.87×10^{15}	2.74×10^{14}	14.1
$0^+ \to 1^-$	4.3872	1	4.00×10^{-5}	1.30×10^{-4}	1.94×10^{19}	5.50×10^{18}	3.52
$0^+ \to 0^+$	4.2605	0	2.60×10^{-5}	7.53×10^{-4}	2.98×10^{19}	9.47×10^{17}	31.5
$0^+ \to 2^+$	4.2178	2	7.00×10^{-6}	2.78×10^{-4}	1.11×10^{20}	2.56×10^{18}	43.2
$^{235}_{92}U \to ^{231}_{90}Th$							
$7/2^- \to 5/2^+$	4.7161	1	5.00	13.70	4.44×10^{17}	9.83×10^{16}	4.52
$7/2^- \to 7/2^+$	4.6741	1	4.20	6.61	5.29×10^{17}	2.04×10^{17}	2.60
$7/2^- \to 9/2^+$	4.6200	1	1.70	2.55	1.31×10^{18}	5.28×10^{17}	2.48
$7/2^- \to 11/2^+$	4.5541	3	0.70	0.62	3.17×10^{18}	2.16×10^{18}	1.47
$7/2^- \to 5/2^-$	4.5304	2	2.10	31.00	1.06×10^{18}	4.34×10^{16}	24.4
$7/2^- \to 7/2^-$	4.5108	0	55.00	24.80	4.04×10^{16}	5.43×10^{16}	0.74
$7/2^- \to 3/2^+$	4.4947	3	0.16	0.21	1.39×10^{19}	6.43×10^{18}	2.16
$7/2^- \to 9/2^-$	4.4792	2	17.00	12.00	1.31×10^{17}	1.12×10^{17}	1.17
$7/2^- \to 5/2^+$	4.4753	1	0.24	0.18	9.26×10^{18}	7.36×10^{18}	1.26
$7/2^- \to 7/2^+$	4.4409	1	0.21	9.58×10^{-2}	1.06×10^{19}	1.40×10^{19}	0.75
$7/2^- \to (11/2^-)$	4.4381	2	4.40	5.56	5.05×10^{17}	2.42×10^{17}	2.09
$7/2^- \to (5/2)^+$	4.4144	1	9.00×10^{-3}	5.80×10^{-2}	2.47×10^{20}	2.32×10^{19}	10.6
$7/2^- \to 5/2^+$	4.3990	1	0.10	0.04	2.22×10^{19}	3.12×10^{19}	0.71
$7/2^- \to (9/2)^+$	4.3912	1	3.30×10^{-2}	3.72×10^{-2}	6.73×10^{19}	3.62×10^{19}	1.86
$7/2^- \to (13/2^-)$	4.3851	4	0.40	1.47	5.55×10^{18}	9.14×10^{17}	6.08
$7/2^- \to (7/2^+)$	4.3386	1	0.90	1.34×10^{-2}	2.47×10^{18}	1.00×10^{20}	2.46×10^{-2}
$7/2^- \to (11/2^+)$	4.3304	3	1.70×10^{-2}	9.07×10^{-3}	1.31×10^{20}	1.48×10^{20}	0.88
$7/2^- \to 7/2^-$	4.3284	0	5.70	0.77	3.90×10^{17}	1.75×10^{18}	0.22
$7/2^- \to 9/2^-$	4.2639	2	0.90	0.19	2.47×10^{18}	7.23×10^{18}	0.34
$7/2^- \to (11/2^-)$	4.1851	2	0.02	3.70×10^{-2}	1.11×10^{20}	3.61×10^{19}	3.08
$7/2^- \to 7/2^-$	4.0821	0	1.00×10^{-3}	4.88×10^{-3}	2.22×10^{21}	2.76×10^{20}	8.06

TABLE II. (*Continued.*)

Transition	Q	$\ell_{\min}$	$B^{\mathrm{exp}}(\%)$	$B^{\mathrm{theor}}(\%)$	$T_{1/2}^{\mathrm{exp}}(\mathrm{s})$	$T_{1/2}^{\mathrm{theor}}(\mathrm{s})$	HF
${}^{236}_{92}\mathrm{U} \to {}^{232}_{90}\mathrm{Th}$							
$0^+ \to 0^+$	4.6109	0	74.00	71.50	9.99×10^{14}	1.08×10^{15}	0.93
$0^+ \to 2^+$	4.5614	2	26.00	26.00	2.84×10^{15}	2.97×10^{15}	0.96
$0^+ \to 4^+$	4.4486	4	0.15	2.44	4.93×10^{17}	3.17×10^{16}	15.5
$0^+ \to 6^+$	4.2775	6	1.40×10^{-4}	5.58×10^{-2}	5.28×10^{20}	1.38×10^{18}	3.82×10^{2}
${}^{238}_{92}\mathrm{U} \to {}^{234}_{90}\mathrm{Th}$							
$0^+ \to 0^+$	4.3078	0	79.00	74.10	1.78×10^{17}	4.10×10^{17}	0.43
$0^+ \to 2^+$	4.2582	2	21.00	24.10	6.71×10^{17}	1.26×10^{18}	0.53
$0^+ \to 4^+$	4.1448	4	7.8×10^{-2}	1.72	1.81×10^{20}	1.77×10^{19}	10.2
${}^{234}_{94}\mathrm{Pu} \to {}^{230}_{92}\mathrm{U}$							
$0^+ \to 0^+$	6.3491	0	68.30	61.70	7.73×10^{5}	3.73×10^{5}	2.07
$0^+ \to 2^+$	6.2974	2	31.70	31.60	1.67×10^{6}	7.28×10^{5}	2.29
$0^+ \to 4^+$	6.1796	4	0.40	6.68	1.32×10^{8}	3.45×10^{6}	38.3
${}^{236}_{94}\mathrm{Pu} \to {}^{232}_{92}\mathrm{U}$							
$0^+ \to 0^+$	5.9062	0	69.10	62.10	1.31×10^{8}	5.71×10^{7}	2.29
$0^+ \to 2^+$	5.8586	2	30.80	31.20	2.93×10^{8}	1.14×10^{8}	2.57
$0^+ \to 4^+$	5.7497	4	0.23	6.20	3.92×10^{10}	5.72×10^{8}	68.6
$0^+ \to 6^+$	5.5835	6	1.85×10^{-3}	0.48	4.88×10^{12}	7.41×10^{9}	6.58×10^{2}
$0^+ \to 8^+$	5.3655	8	1.30×10^{-5}	1.37×10^{-2}	6.94×10^{14}	2.58×10^{11}	2.69×10^{3}
$0^+ \to 1^-$	5.3430	1	2.60×10^{-4}	4.81×10^{-4}	3.47×10^{13}	7.37×10^{12}	4.71
$0^+ \to 0^+$	5.2147	0	5.80×10^{-4}	5.04×10^{-3}	1.56×10^{13}	7.03×10^{11}	22.1
$0^+ \to 2^+$	5.1716	2	1.30×10^{-5}	2.36×10^{-3}	6.94×10^{14}	1.50×10^{12}	4.61×10^{2}
$0^+ \to 5^-$	5.1594	5	2.46×10^{-6}	1.91×10^{-5}	3.67×10^{15}	1.86×10^{14}	19.7
$0^+ \to 4^+$	5.0727	4	6.00×10^{-7}	3.97×10^{-4}	1.50×10^{16}	8.93×10^{12}	1.68×10^{3}
$0^+ \to 2^+$	5.0393	2	1.21×10^{-5}	3.02×10^{-4}	7.45×10^{14}	1.18×10^{13}	63.4
$0^+ \to (0^+)$	4.9789	0	1.33×10^{-5}	1.28×10^{-4}	6.78×10^{14}	2.77×10^{13}	24.5
$0^+ \to (2^+)$	4.9386	2	1.53×10^{-5}	5.96×10^{-5}	5.89×10^{14}	5.95×10^{13}	9.91
${}^{238}_{94}\mathrm{Pu} \to {}^{234}_{92}\mathrm{U}$							
$0^+ \to 0^+$	5.6322	0	70.90	62.00	3.90×10^{9}	1.83×10^{09}	2.13
$0^+ \to 2^+$	5.5887	2	28.98	31.20	9.55×10^{9}	3.63×10^{09}	2.63
$0^+ \to 4^+$	5.4888	4	0.11	6.28	2.64×10^{12}	1.81×10^{10}	1.46×10^{2}
$0^+ \to 6^+$	5.3361	6	3.00×10^{-3}	0.492	9.23×10^{13}	2.31×10^{11}	4.00×10^{2}
$0^+ \to 8^+$	5.1352	8	6.80×10^{-6}	1.44×10^{-2}	4.07×10^{16}	7.88×10^{12}	5.17×10^{3}
$0^+ \to 1^-$	4.8459	1	2.20×10^{-5}	6.89×10^{-6}	1.26×10^{16}	1.65×10^{16}	0.76
$0^+ \to 0^+$	4.8223	0	5.00×10^{-5}	3.22×10^{-4}	5.54×10^{15}	3.53×10^{14}	15.7
$0^+ \to 3^-$	4.7829	3	9.00×10^{-8}	1.95×10^{-6}	3.08×10^{18}	5.81×10^{16}	52.9
$0^+ \to 2^+$	4.7805	2	5.93×10^{-6}	1.41×10^{-4}	4.67×10^{16}	8.07×10^{14}	57.9
$0^+ \to 2^+$	4.7055	2	1.20×10^{-5}	3.81×10^{-5}	2.31×10^{16}	2.98×10^{15}	7.74
$0^+ \to 4^+$	4.6846	4	2.50×10^{-7}	2.02×10^{-5}	1.11×10^{18}	5.62×10^{15}	1.97×10^{2}
$0^+ \to 2^-$	4.6428	3	7.00×10^{-8}	1.66×10^{-7}	3.95×10^{18}	6.85×10^{17}	5.77
$0^+ \to 3^-$	4.6083	3	0.00	8.87×10^{-8}	–	1.28×10^{18}	–
$0^+ \to 0^-$	4.5877	1	1.20×10^{-6}	7.38×10^{-8}	2.31×10^{17}	1.54×10^{18}	0.15
$0^+ \to 2^+$	4.5469	2	1.10×10^{-6}	2.15×10^{-6}	2.52×10^{17}	5.27×10^{16}	4.77
${}^{240}_{94}\mathrm{Pu} \to {}^{236}_{92}\mathrm{U}$							
$0^+ \to 0^+$	5.2948	0	72.80	65.00	2.84×10^{11}	1.93×10^{11}	1.47
$0^+ \to 2^+$	5.2496	2	27.10	30.00	7.64×10^{11}	4.18×10^{11}	1.83
$0^+ \to 4^+$	5.1453	4	8.4×10^{-2}	4.83	2.46×10^{14}	2.60×10^{12}	95.0
$0^+ \to 6^+$	4.9850	6	1.06×10^{-3}	0.26	1.95×10^{16}	4.81×10^{13}	4.06×10^{2}
$0^+ \to 8^+$	4.7725	8	4.60×10^{-5}	4.32×10^{-3}	4.50×10^{17}	2.90×10^{15}	1.55×10^{2}
$0^+ \to 1^-$	4.6072	1	2.00×10^{-5}	1.23×10^{-5}	1.04×10^{18}	1.02×10^{18}	1.02
$0^+ \to 3^-$	4.5506	3	1.30×10^{-8}	3.59×10^{-6}	1.59×10^{21}	3.49×10^{18}	4.57×10^{2}
$0^+ \to 0^+$	4.3756	0	5.90×10^{-7}	1.07×10^{-5}	3.51×10^{19}	1.17×10^{18}	29.9

TABLE II. (*Continued.*)

Transition	Q	ℓ_{min}	$B^{exp}(\%)$	$B^{theor}(\%)$	$T_{1/2}^{exp}(s)$	$T_{1/2}^{theor}(s)$	HF
$0^+ \to (2^+)$	4.3368	2	5.00×10^{-8}	4.39×10^{-6}	4.14×10^{20}	2.86×10^{18}	1.45×10^{2}
$0^+ \to (2^+)$	4.3348	2	2.50×10^{-8}	4.21×10^{-6}	8.28×10^{20}	2.97×10^{18}	2.79×10^{2}
$0^+ \to 1^-$	4.3278	1	2.50×10^{-8}	5.92×10^{-8}	8.28×10^{20}	2.12×10^{20}	3.91
${}^{242}_{94}Pu \to {}^{238}_{92}U$							
$0^+ \to 0^+$	5.0235	0	76.49	67.20	1.54×10^{13}	2.87×10^{13}	0.54
$0^+ \to 2^+$	4.9786	2	23.48	28.70	5.02×10^{13}	6.72×10^{13}	0.75
$0^+ \to 4^+$	4.8751	4	0.03	3.88	3.84×10^{16}	4.98×10^{14}	77.1
$0^+ \to 6^+$	4.7163	6	8.60×10^{-4}	0.16	1.37×10^{18}	1.22×10^{16}	1.12×10^{2}
${}^{244}_{94}Pu \to {}^{240}_{92}U$							
$0^+ \to 0^+$	4.7052	0	80.60	71.50	3.18×10^{15}	6.37×10^{15}	0.50
$0^+ \to (2^+)$	4.6612	2	19.40	28.50	1.32×10^{16}	1.60×10^{16}	0.83
${}^{238}_{96}Cm \to {}^{234}_{94}Pu$							
$0^+ \to 0^+$	6.6654	0	69.53	64.20	3.24×10^{5}	1.83×10^{5}	1.76
$0^+ \to 2^+$	6.6194	2	30.47	35.80	7.38×10^{5}	3.29×10^{5}	2.25
${}^{240}_{96}Cm \to {}^{236}_{94}Pu$							
$0^+ \to 0^+$	6.4380	0	71.10	58.80	3.29×10^{6}	1.95×10^{6}	1.69
$0^+ \to 2^+$	6.3934	2	28.90	32.40	8.10×10^{6}	3.54×10^{6}	2.29
$0^+ \to 4^+$	6.2905	4	0.05	7.96	4.50×10^{9}	1.44×10^{7}	3.13×10^{2}
$0^+ \to 6^+$	6.1322	6	1.40×10^{-2}	0.86	1.67×10^{10}	1.34×10^{8}	1.25×10^{2}
${}^{242}_{96}Cm \to {}^{238}_{94}Pu$							
$0^+ \to 0^+$	6.2559	0	74.08	59.00	1.90×10^{7}	7.32×10^{6}	2.60
$0^+ \to 2^+$	6.2118	2	25.92	32.30	5.43×10^{7}	1.34×10^{7}	4.07
$0^+ \to 4^+$	6.1099	4	3.50×10^{-2}	7.85	4.02×10^{10}	5.50×10^{7}	7.32×10^{2}
$0^+ \to 6^+$	5.9525	6	4.60×10^{-3}	0.82	3.06×10^{11}	5.27×10^{8}	5.81×10^{2}
$0^+ \to 8^+$	5.7423	8	2.00×10^{-5}	3.45×10^{-2}	7.04×10^{13}	1.25×10^{10}	5.62×10^{3}
$0^+ \to 1^-$	5.6508	1	2.50×10^{-4}	4.40×10^{-4}	5.63×10^{12}	9.81×10^{11}	5.74
$0^+ \to 3^-$	5.5946	3	1.26×10^{-5}	1.74×10^{-4}	1.12×10^{14}	2.49×10^{12}	44.9
$0^+ \to 5^-$	5.4927	5	2.20×10^{-7}	3.12×10^{-5}	6.40×10^{15}	1.38×10^{13}	4.62×10^{2}
$0^+ \to 0^+$	5.3145	0	3.60×10^{-5}	2.56×10^{-4}	3.91×10^{13}	1.69×10^{12}	23.2
$0^+ \to 1^-$	5.2932	1	1.13×10^{-6}	2.68×10^{-6}	1.25×10^{15}	1.61×10^{14}	7.73
$0^+ \to 2^+$	5.2729	2	1.70×10^{-6}	1.24×10^{-4}	8.28×10^{14}	3.49×10^{12}	2.37×10^{2}
$0^+ \to 2^+$	5.2273	2	3.70×10^{-6}	6.18×10^{-5}	3.80×10^{14}	6.99×10^{12}	54.4
$0^+ \to (4^+)$	5.1301	4	3.10×10^{-7}	1.07×10^{-5}	4.54×10^{15}	4.03×10^{13}	1.13×10^{2}
$0^+ \to 0^+$	5.0272	0	5.50×10^{-7}	2.91×10^{-6}	2.56×10^{15}	1.48×10^{14}	1.73
$0^+ \to 2^+$	4.9916	2	5.20×10^{-7}	1.46×10^{-6}	2.71×10^{15}	2.95×10^{14}	9.17
${}^{244}_{96}Cm \to {}^{240}_{94}Pu$							
$0^+ \to 0^+$	5.9420	0	76.90	60.30	7.43×10^{8}	3.70×10^{8}	2.01
$0^+ \to 2^+$	5.8992	2	23.10	31.90	2.47×10^{9}	6.99×10^{8}	3.54
$0^+ \to 4^+$	5.8003	4	0.02	7.14	2.80×10^{12}	3.12×10^{9}	8.97×10^{2}
$0^+ \to 6^+$	5.6477	6	3.52×10^{-3}	0.65	1.62×10^{13}	3.41×10^{10}	4.76×10^{2}
$0^+ \to 8^+$	5.4445	8	4.00×10^{-5}	2.3×10^{-2}	1.43×10^{15}	9.66×10^{11}	1.48×10^{3}
$0^+ \to 1^-$	5.3447	1	5.60×10^{-5}	2.55×10^{-4}	1.02×10^{15}	8.73×10^{13}	11.7
$0^+ \to 3^-$	5.2931	3	4.00×10^{-6}	9.94×10^{-5}	1.43×10^{16}	2.24×10^{14}	63.7
$0^+ \to 0^+$	5.0813	0	1.49×10^{-4}	3.08×10^{-4}	3.84×10^{14}	7.23×10^{13}	5.30
$0^+ \to 2^+$	5.0417	2	5.00×10^{-5}	1.46×10^{-4}	1.14×10^{15}	1.53×10^{14}	7.49
${}^{246}_{96}Cm \to {}^{242}_{94}Pu$							
$0^+ \to 0^+$	5.5154	0	82.20	67.60	1.83×10^{11}	1.26×10^{11}	1.45
$0^+ \to 2^+$	5.4709	2	17.80	32.40	8.44×10^{11}	2.64×10^{11}	3.19
${}^{248}_{96}Cm \to {}^{244}_{94}Pu$							
$0^+ \to 0^+$	5.2013	0	81.90	66.20	1.46×10^{13}	1.37×10^{13}	1.07
$0^+ \to 2^+$	5.1571	2	18.03	29.70	6.65×10^{13}	3.06×10^{13}	2.17
$0^+ \to 4^+$	5.0463	4	7.60×10^{-2}	3.91	1.57×10^{16}	2.33×10^{14}	67.4
$0^+ \to 6^+$	4.8834	6	5.46×10^{-3}	0.17	2.20×10^{17}	5.32×10^{15}	41.2

TABLE II. (*Continued.*)

Transition	Q	ℓ_{min}	$B^{exp}(\%)$	$B^{theor}(\%)$	$T_{1/2}^{exp}(s)$	$T_{1/2}^{theor}(s)$	HF
${}^{244}_{98}Cf \to {}^{240}_{96}Cm$							
$0^+ \to 0^+$	7.3705	0	75.70	60.60	2.20×10^3	1.25×10^3	1.76
$0^+ \to (2^+)$	7.3325	2	25.70	39.40	6.47×10^3	1.92×10^3	3.37
${}^{246}_{98}Cf \to {}^{242}_{96}Cm$							
$0^+ \to 0^+$	6.9032	0	79.30	55.60	1.62×10^5	1.18×10^5	1.37
$0^+ \to 2^+$	6.8611	2	20.60	33.00	6.24×10^5	1.99×10^5	3.14
$0^+ \to 4^+$	6.7662	4	0.15	9.96	8.57×10^7	6.58×10^5	1.30×10^2
$0^+ \to 6^+$	6.6152	6	1.60×10^{-2}	1.41	8.03×10^8	4.64×10^6	1.73×10^2
${}^{248}_{98}Cf \to {}^{244}_{96}Cm$							
$0^+ \to 0^+$	6.4030	0	80.00	59.10	3.60×10^7	2.34×10^7	1.54
$0^+ \to 2^+$	6.3600	2	19.60	32.70	1.47×10^8	4.24×10^7	3.47
$0^+ \to 4^+$	6.2607	4	0.40	8.15	7.20×10^9	1.70×10^8	42.3
${}^{250}_{98}Cf \to {}^{246}_{96}Cm$							
$0^+ \to 0^+$	6.1701	0	84.70	60.10	4.88×10^8	4.85×10^8	1.01
$0^+ \to 2^+$	6.1272	2	15.00	32.00	2.75×10^9	9.12×10^8	3.02
$0^+ \to 4^+$	6.0281	4	0.30	7.25	1.38×10^{11}	4.02×10^9	34.2
$0^+ \to 6^+$	5.8752	6	0.01	0.68	4.13×10^{12}	4.29×10^{10}	96.2
${}^{252}_{98}Cf \to {}^{248}_{96}Cm$							
$0^+ \to 0^+$	6.2586	0	84.20	60.00	1.02×10^8	1.99×10^8	0.51
$0^+ \to 2^+$	6.2152	2	15.70	32.00	5.49×10^8	3.74×10^8	1.47
$0^+ \to 4^+$	6.1150	4	0.24	7.27	3.63×10^{10}	1.64×10^9	22.1
$0^+ \to 6^+$	5.9605	6	2.00×10^{-3}	0.69	4.31×10^{12}	1.74×10^{10}	2.48×10^2
$0^+ \to 8^+$	5.7536	8	5.99×10^{-5}	2.50×10^{-2}	1.44×10^{14}	4.77×10^{11}	3.02×10^2
${}^{248}_{100}Fm \to {}^{244}_{98}Cf$							
$0^+ \to 0^+$	8.0449	0	79.60	60.20	48.6	35.2	1.38
$0^+ \to 2^+$	8.0039	2	20.00	39.80	1.94×10^2	53.2	3.64
${}^{250}_{100}Fm \to {}^{246}_{98}Cf$							
$0^+ \to 0^+$	7.6003	0	83.30	61.90	2.64×10^3	1.83×10^3	1.44
$0^+ \to (2^+)$	7.5563	2	16.70	38.10	1.32×10^4	2.97×10^3	4.44
${}^{252}_{100}Fm \to {}^{248}_{98}Cf$							
$0^+ \to 0^+$	7.1950	0	84.00	55.20	1.09×10^5	9.31×10^4	1.17
$0^+ \to 2^+$	7.1535	2	15.00	33.20	6.09×10^5	1.55×10^5	3.94
$0^+ \to 4^+$	7.0572	4	0.97	10.10	9.42×10^6	5.11×10^5	18.4
$0^+ \to 6^+$	6.9100	6	2.30×10^{-2}	1.53	3.97×10^8	3.36×10^6	1.18×10^2
${}^{252}_{102}No \to {}^{248}_{100}Fm$							
$0^+ \to 0^+$	8.5943	0	75.90	60.10	5.16	3.92	1.32
$0^+ \to 2^+$	8.5503	2	24.10	39.90	16.2	5.91	2.75

the orbital momentum. For transitions with $\ell = 5, 6$ the HF increases and reaches the values 10^2–10^3.

Note that the values of the HF for several α-decay transitions presented in Table II are close to $\sim 10^{-2}$. The parities of parent and daughter nuclei are different for such transitions. The probability of parent nucleus representation as an α particle and daughter nucleus in a specific excited state is drastically increased for these cases. The reason for such transition acceleration is difficult to understand in the framework of the cluster approach. Therefore additional microscopic studies of these cases are required.

The values of the branching ratios evaluated in the framework of our model and other approaches [7,20,25] are compared with experimental data in Table III. Note that the same set of parameters for the ground-state-to-ground-state and the ground-state-to-excited-state α transitions is used in our model. In contrast, one additional fitting parameter has been introduced in Refs. [20,25] for description of the same data. Moreover, the one extra fitting parameter (μ) is used for each value of the orbital momentum $\ell = 1, 2, 3, 4$ [7]. The supplementary fitting parameters give the possibility of obtaining values of the branch ratios, which are very close to the experimental ones.

From the results presented in Table II, we see that the low-lying even-parity levels of the daughter nucleus rotational band, built on the ground state, are well described. The higher

TABLE III. The comparison table of the experimental and theoretical branch ratio values.

Transition	Q	$\ell_{\min}$	$B^{\exp}(\%)$	$B(\%)$	B [25](%)	B [20](%)	B [7](%)
$^{238}_{94}Pu \to ^{234}_{92}U$							
$0^+ \to 0^+$	5.6322	0	70.90	62.00	75.57	77.41	70.99
$0^+ \to 2^+$	5.5887	2	28.98	31.20	23.00	21.52	4.84
$0^+ \to 4^+$	5.4888	4	0.11	6.28	1.41	1.06	0.214
$0^+ \to 6^+$	5.3361	6	3.00×10^{-3}	0.492	1.76×10^{-2}	9.30×10^{-3}	–
$0^+ \to 8^+$	5.1352	8	6.80×10^{-6}	1.44×10^{-2}	4.40×10^{-5}	1.41×10^{-5}	–
$0^+ \to 0^+$	4.8223	0	5.00×10^{-5}	3.22×10^{-4}	3.65×10^{-5}	8.00×10^{-5}	6.05×10^{-5}
$0^+ \to 0^-$	4.5877	1	1.20×10^{-6}	7.38×10^{-8}	2.89×10^{-7}	9.00×10^{-7}	1.30×10^{-6}
$^{242}_{96}Cm \to ^{238}_{94}Pu$							
$0^+ \to 0^+$	6.2559	0	74.08	59.00	74.00	76.0	74.09
$0^+ \to 2^+$	6.2118	2	25.92	32.30	24.20	22.70	36.21
$0^+ \to 4^+$	6.1099	4	3.50×10^{-2}	7.85	1.765	1.333	0.45
$0^+ \to 6^+$	5.9525	6	4.60×10^{-3}	0.82	0.28×10^{-2}	1.52×10^{-2}	–
$0^+ \to 8^+$	5.7423	8	2.00×10^{-5}	3.45×10^{-2}	1.00×10^{-4}	3.2×10^{-5}	–
$^{246}_{98}Cf \to ^{242}_{96}Cm$							
$0^+ \to 0^+$	6.9032	0	79.30	55.90	71.60	73.90	79.28
$0^+ \to 2^+$	6.8611	2	20.60	33.00	25.90	24.30	22.66
$0^+ \to 4^+$	6.7662	4	0.15	9.79	2.43	1.82	1.04
$0^+ \to 6^+$	6.6152	6	1.60×10^{-2}	1.35	6.10×10^{-2}	3.20×10^{-2}	–

exited even/odd-parity levels are described worse, but we can estimate the hindrance factor.

V. CONCLUSIONS

In the framework of our model, we can describe simultaneously the ground-state-to-ground-state and the ground-state-to-excited-state α transitions as well as the α-capture cross section around the barrier in a wide range of nuclei mass numbers. The experimental data for spins, parities, mass excesses, excitation energy of excited state in daughter nucleus, and branching ratio values between various decay modes (α, β, etc.) are taken into account in our model. The energies released in α decay and angular momenta of the emitted α particle are mainly determined by the branching ratio between the ground-state-to-ground-state and the ground-state-to-excited-state α transitions, see Eqs. (3), (4), and (14). The branching ratio is strongly reduced for states with increasing value of ℓ due to centrifugal potential contribution into the action [the action is defined by the integral in Eq. (4)]. The α transitions into high excited states are also suppressed, because the value of action rises due to the reduction of the energy released in α decay.

As a rule, we obtain good agreement for transitions with $\ell = 0$ and $\ell = 2$. The transitions into high exited states are described worse because of the influence of nuclear structure and other effects on α-particle formation. However, we can estimate the hindrance factor, which estimates the influence of other effects on α decay.

[1] NuDat2.4, http://www.nndc.bnl.gov (last update July 15, 2008).
[2] G. Audi, O. Bersillon, J. Blachot, and A. H. Wapstra, Nucl. Phys. **A729**, 3 (2003).
[3] http://www-nds.iaea.org/RIPL-2/.
[4] *Table of Isotopes*, 8th ed., edited by R. Firestone and V. Shirley (Wiley, New York, 1996).
[5] G. Gamow, Z. Phys. **51**, 204 (1928).
[6] G. Gamow and C. L. Critchfield, *Theory of Atomic Nucleus and Nuclear Energy Sources* (Clarendon, Oxford, 1949).
[7] M. A. Preston, Phys. Rev. **71**, 865 (1947).
[8] P. Möller, J. R. Nix, and K.-L. Kratz, At. Data Nucl. Data Tables **66**, 131 (1997).
[9] R. Moustabchir and G. Royer, Nucl. Phys. **A683**, 266 (2001).
[10] M. Fujiwara, T. Kawabata, and P. Mohr, J. Phys. G **28**, 643 (2002).
[11] M. Gupta and T. W. Burrows, Nucl. Data Sheets **106**, 251 (2005).
[12] V. Yu. Denisov and H. Ikezoe, Phys. Rev. C **72**, 064613 (2005).
[13] D. N. Poenaru, I.-H. Plonski, and W. Greiner, Phys. Rev. C **74**, 014312 (2006).
[14] E. L. Medeiros, M. M. N. Rodrigues, S. B. Duarte, and O. A. P. Tavares, J. Phys. G **32**, B23 (2006).
[15] N. Dasgupta-Schubert and M. A. Reyes, At. Data Nucl. Data Tables **93**, 907 (2007).
[16] A. Sobiczewski and A. Parkhomenko, Phys. At. Nucl. **69**, 1155 (2006).
[17] V. Yu. Denisov and A. A. Khudenko, At. Data Nucl. Data Tables (2009) doi:10.1016/j.adt.2009.06.003; Phys. Rev. C **79**, 054614 (2009).
[18] V. Yu. Denisov and A. A. Khudenko, Nucl. Phys. At. Energy **3**, 33 (2008); in *Proceedings of the Second International Conference on Current Problems in Nuclear Physics and Atomic Energy (NPAE-Kiev2008), 9–15 June 2008* (Kiev, Ukraine, 2008), p. 438.

[19] Chang Xu and Zhongzhou Ren, Phys. Rev. C **75**, 044301 (2007).
[20] Chang Xu and Zhongzhou Ren, Nucl. Phys. **A778**, 1 (2006).
[21] B. Buck, A. C. Merchant, and S. M. Perez, Phys. Rev. C **51**, 559 (1995); B. Buck, J. C. Johnston, A. C. Merchant, and S. M. Perez, *ibid.* **52**, 1840 (1995); B. Buck, A. C. Merchant, and S. M. Perez, *ibid.* **54**, 2063 (1996).
[22] D. S. Delion, S. Peltonen, and J. Suhonen, Phys. Rev. C **73**, 014315 (2006).
[23] S. Peltonen, D. S. Delion, and J. Suhonen, Phys. Rev. C **78**, 034608 (2008).
[24] Xiaoping Zhang and Zhongzhou Ren, J. Phys. G **31**, 959 (2005).
[25] Y. Z. Wang, H. F. Zhang, J. M. Dong, and G. Royer, Phys. Rev. C **79**, 014316 (2009).
[26] D. S. Delion, A. Insolia, and R. J. Liotta, Phys. Rev. C **49**, 3024 (1994).
[27] J. Gasparro, G. Ardisson, V. Barci, and R. K. Sheline, Phys. Rev. C **62**, 064305 (2000).
[28] K.-N. Huang, M. Aoyagi, M. H. Chen, B. Crasemann, and H. Mark, At. Data Nucl. Data Tables **18**, 243 (1976).